

Received 10 June 2025, accepted 18 July 2025, date of publication 24 July 2025, date of current version 30 July 2025.

Digital Object Identifier 10.1109/ACCESS.2025.3592338



Machine Learning Approach to Aerodynamic Analysis of NACA0005 Airfoil: ANN and CFD Integration

TAIBA KOUSER[®]¹, DILEK FUNDA KURTULUS[®]², SRIKANTH GOLI[®]¹, ABDULRAHMAN ALIYU[®]¹, IMIL HAMDA IMRAN[®]³, LUAI M. ALHEMS¹, AND AZHAR M. MEMON[®]¹

Applied Research Center for Metrology, Standards and Testing, King Fahd University of Petroleum and Minerals (KFUPM), Dhahran 31261, Saudi Arabia

Corresponding author: Taiba Kouser (taiba.kouser@kfupm.edu.sa)

This work was supported in part by the Applied Research Centre for Metrology Standards and Testing, King Fahd University of Petroleum and Minerals (KFUPM); and in part by the Research, Development, and Innovation Authority (RDIA), Saudi Arabia, under Project 12922-KFUPM-2023-KFUPM-R-3-1-EI. The work of Imil Hamda Imran was supported by the Deanship of Scientific Research, Vice Presidency for Graduate Studies and Scientific Research, King Faisal University, Saudi Arabia, under Grant KFU252639.

ABSTRACT This study presents a machine learning approach to predict the unsteady aerodynamic performance of a NACA0005 airfoil. Data generated by computational fluid dynamics (CFD) is used to train the model for Reynolds numbers $Re \in [1000 - 5000]$ and angles of attack ranging from 9° to 11°. A robust Scaled Conjugate Gradient (SCG) algorithm is employed for efficient training of data. The ANN has a two-layer architecture, 9 fixed neurons in the first hidden layer and a varying number of neurons in the second layer to achieve optimal performance. The model yielded coefficients of determination (R^2) of 0.994 (Coefficient of lift (C_l)) and 0.9615 (Coefficient of drag (C_d)) for training, and 0.9563 (C_l) and 0.9085 (C_d) for testing. Overall mean errors are found to be less than 1%. It offers a powerful surrogate modeling approach for aerodynamic studies at ultra-low Reynolds numbers. Moreover, it provides rapid and reliable alternatives to traditional CFD simulations in aerodynamic analysis for unseen cases.

INDEX TERMS NACA0005, aerodynamic coefficients, Reynolds number, angle of attack, artificial neural network (ANN).

I. INTRODUCTION

The powerful fitting ability of deep learning has made it widely used in fields such as medical science, chemistry, biology, and so on. Additionally, the ability to model time-series data and extract governing equations has become increasingly important in the world of data analysis. As a result of this capability, researchers can not only examine underlying phenomena, but also generate data-driven predictions. It allows them to uncover large-scale patterns and hidden structures within the datasets [1], [2], [3], [4]. In general, aerodynamic modeling methods fall into two categories (i) physics-based models and (ii) data-driven models. Due to

The associate editor coordinating the review of this manuscript and approving it for publication was Rosario Pecora.

close relationship between physics-based models [5], [6], [7] to aerodynamic configurations, these models are physically interpretable. Physics-based models are often insufficiently accurate, particularly when the linear hypothesis no longer holds true for small angles of attack. However, data-driven models are represented by machine learning (ML) models. As computational power has increased, particularly with the development of more efficient hardware (GPUs and memory storage), the development of open-source machine learning communities, and user-friendly software, has become more powerful.

Artificial neural network (ANN) has gained high attention in recent years as an effective tool for tackling fluid mechanics problems [8], [9], [10]. Brunton et al. [8] divide machine learning in fluid mechanics into two main areas:

²Aerospace Engineering Department, Middle East Technical University (METU), 06800 Ankara, Türkiye

³Department of Electrical Engineering, College of Engineering, King Faisal University, Al Ahsa 31982, Saudi Arabia



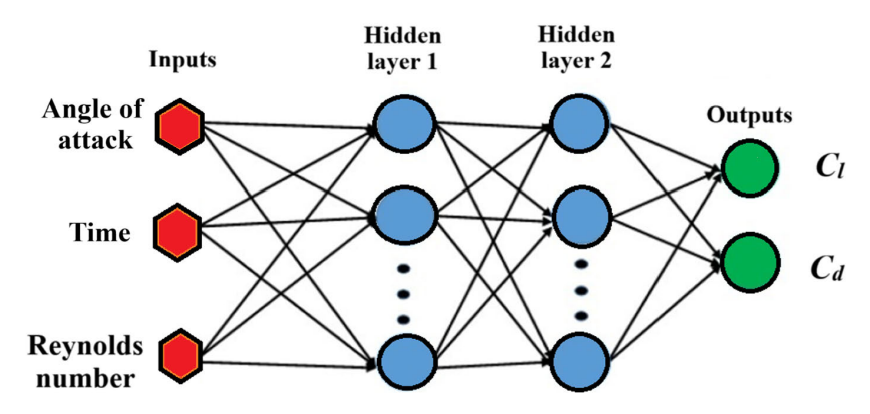


FIGURE 1. ANN architecture for unsteady lift and drag coefficients.

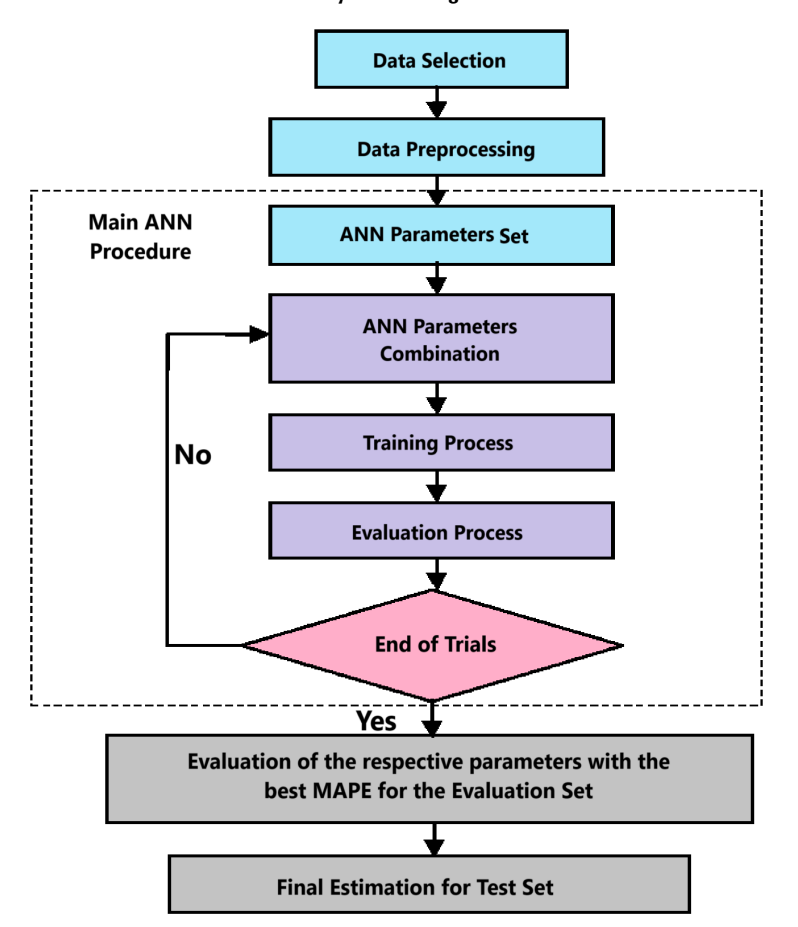


FIGURE 2. Methodology flowchart for evaluating lift and drag coefficients using ANN.

feature extraction and modeling flow dynamics. Machine learning was first implemented in fluid mechanics in the pioneering work of Greenman and Roth [11] which optimized an airfoil using a neural network. In aerodynamics, airfoil lift coefficient calculations play a crucial role. Machine learning as a control strategy for turbulence and other complex nonlinear systems was introduced by Duriez et al. [12]. Brenner et al. [13] discussed the strengths and limitations of using ML techniques to solve such problems and how they might advance fluid mechanics. Computational fluid dynamics is commonly used to achieve this goal, which

can sometimes be computationally expensive [14], [15], [16]. Recent advances in machine learning and data-driven techniques have made it possible to develop methods to predict aerodynamic coefficients for airfoils, including integral quantities (C_l and C_d), pressure fields (C_p), and unsteady forces [17], [18], [19], [20]. Angles of attack from $0^{\circ} - 9^{\circ}$ were tested for incompressible to transonic flow conditions [17]. Results show that advanced deep learning techniques, such as CNN and GCNN, can predict complex flows more accurately than classical tools. A CNN-based prediction method was proposed by Zhang et al. [21]



TABLE 1. Coefficient of determination (R^2) values for the training and testing of unsteady lift and drag coefficients in case of two-layer neural network. The first layer has 9 neurons and the second varies from 1–100.

| Number of Neurons | $C_l(R^2)$ | | $C_d(R^2)$ | |
|-------------------|------------|-----------|------------|-----------|
| | Training | Predicted | Training | Predicted |
| 3 | 0.9922 | 0.8599 | 0.9862 | 0.8765 |
| 5 | 0.994 | 0.9563 | 0.9615 | 0.9085 |
| 15 | 0.9853 | 0.9006 | 0.9601 | 0.8859 |
| 28 | 0.9726 | 0.942 | 0.9639 | 0.8425 |
| 32 | 0.9753 | 0.9025 | 0.976 | 0.8977 |
| 36 | 0.9845 | 0.9004 | 0.9808 | 0.8816 |
| 45 | 0.9735 | 0.863 | 0.9639 | 0.8503 |
| 59 | 0.9848 | 0.7914 | 0.9779 | 0.8507 |
| 62 | 0.9813 | 0.8808 | 0.9794 | 0.9216 |
| 91 | 0.9871 | 0.7625 | 0.9798 | 0.8963 |

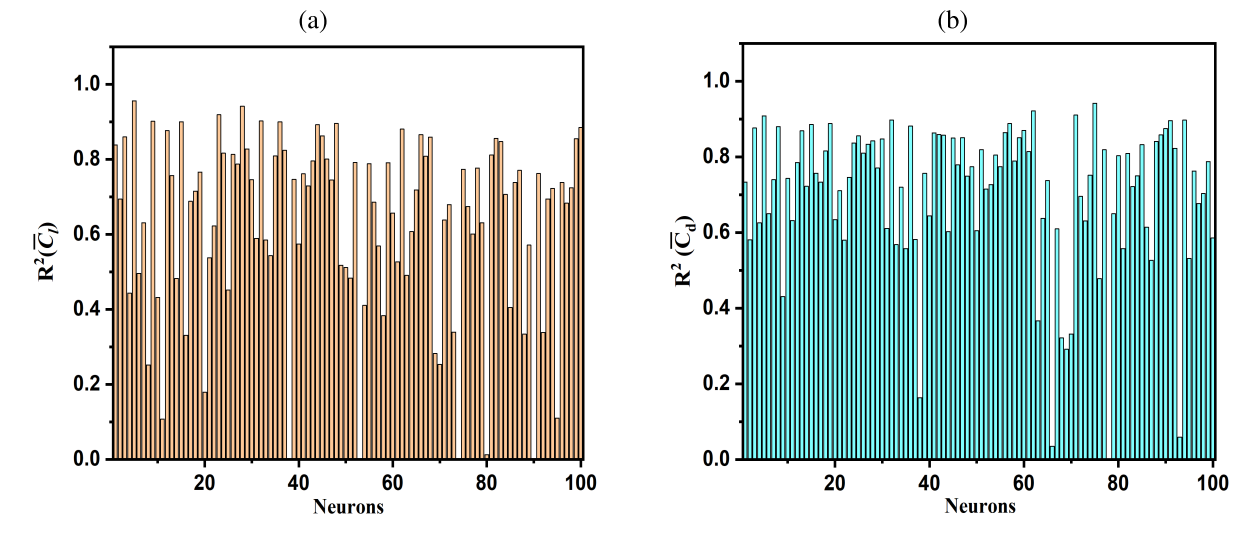


FIGURE 3. Coefficient of determination (R^2) values for predicting (a) lift coefficient (C_I) and (b) drag coefficient (C_d) using a two-layer neural network. The first layer has 9 neurons; the second varies from 1–100. The 5-neuron setup achieved balanced, accurate predictions across both outputs.

for airfoil lift coefficients for different shapes at different free-stream Mach numbers, Reynolds numbers, and angles of attack. Reduced order model has been developed to study unsteady aerodynamics for six-digit NACA series of plunging and pitching motion for airfoils. A deep learning model was developed that accurately predicts aerodynamic forces on airfoils, demonstrating the effectiveness of neural networks to capture complex aerodynamic behaviors.

Machine learning techniques can also be used to forecast flow behavior directly, bypassing or mimicking CFD solvers [22]. Unlike some faster CFD methods that still rely on solving part of the physics, a neural network can be trained to learn all the physics within a certain range of conditions. Consequently, these are designed to work within a predefined parameter space for inputs and outputs. It opens the door to fast optimization processes in multidisciplinary studies. Hybrid CFD-NN method has been used by Ajuria Illarramendi et al. [23] to solve Poisson equation. Based on the flow operating point, the accuracy of the network is found to be affected by the flow operating point on CFD data with known rheologies to simulate previously available flow data.

The present study falls into this category (Hybrid CFD-NN) where the base data set is taken from CFD simulations. Building on the findings of Kouser et al. [24], this study extends their work by leveraging the Scaled Conjugate Gradient (SCG) algorithm to optimize ANN performance. Machine learning approaches for low-thickness airfoils remain to be developed. A distinctive feature of this research is its systematic evaluation of ANN architectures, identifying



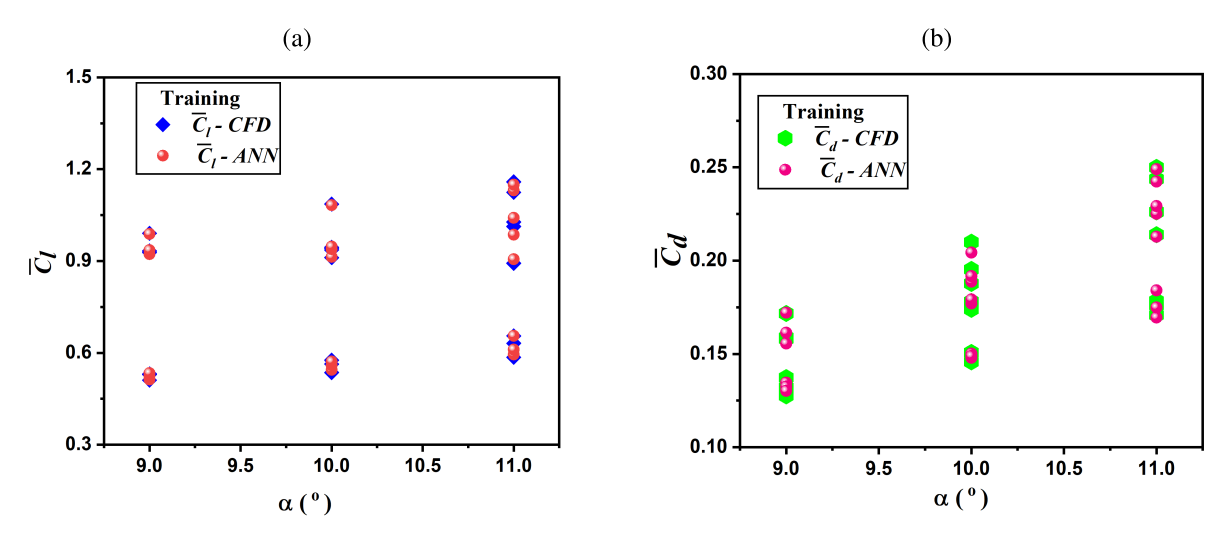


FIGURE 4. Comparative results for CFD values and ANN predictions during the training phase for (a) mean lift coefficient $\overline{C_I}$ and (b) mean drag coefficient $\overline{C_d}$ at different angles of attack.

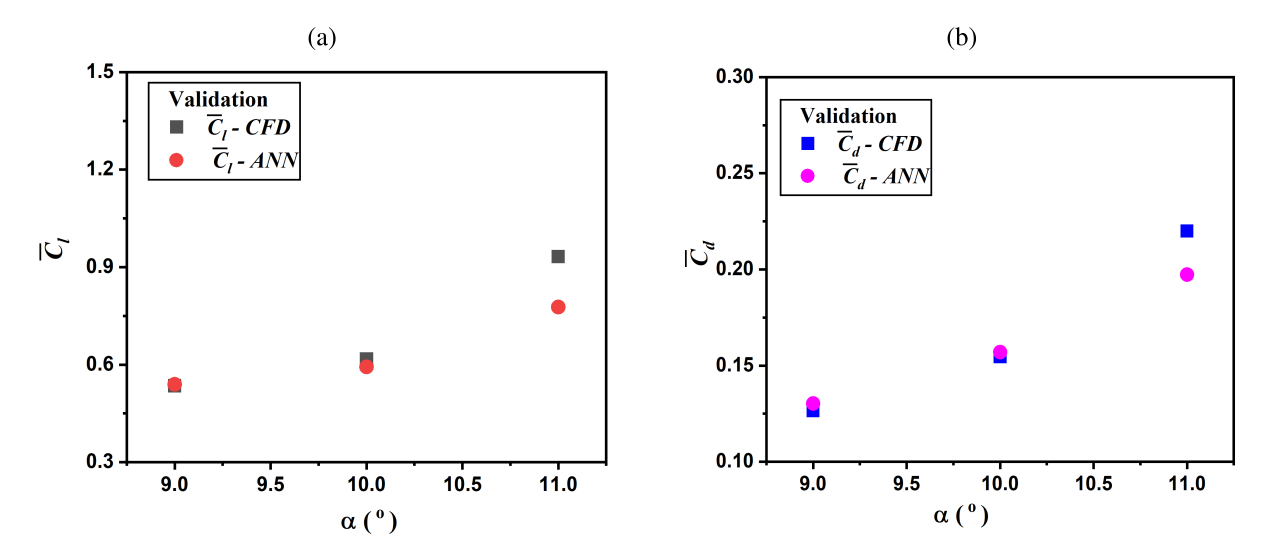


FIGURE 5. Comparing results of CFD and ANN models (a) mean lift coefficient $\overline{C_I}$ and (b) mean drag coefficient $\overline{C_d}$ for different angles of attack α .

an optimal configuration with five neurons in the second hidden layer for a low thickness airfoil NACA0005. This configuration achieves exceptional predictive accuracy, with an R^2 value exceeding 0.90 and a minimal overall prediction error of 1% for both outputs. the effectiveness of the ANN is examined using error metrics, and a comparison with high-fidelity computational fluid dynamics simulations. The goal is to test the accuracy, general performance, and ability of the ANN to handle unsteady aerodynamic behavior at ultra-low Reynolds numbers.

II. METHODOLOGY

A. DATA CLASSIFICATION

In this study, we build the ANN based on the work of Kouser et al. [24]. All simulations were conducted using ANSYS Fluent v22, focusing on NACA 0005 airfoil. The flow regime was characterized by the Reynolds number:

for Re < 2000, a laminar model was used, and for Re > 2000, the $k-\omega$ SST turbulence model was applied to capture transitional and turbulent effects accurately. Based on literature, the CFD-generated dataset is used as ground truth for training and validating machine learning models. The data is trained utilizing the Scaled Conjugate Gradient (SCG) algorithm [25], [26]. The data set includes 28 angles of attack in the range $\alpha \in [9^{\circ} - 11^{\circ}]$, Reynolds numbers $Re \in [1000 - 5000]$, and a normalized time (t/T) from 0 to 1 for one cycle. The three input variables are angles of attack (α) , Reynolds number (Re), and normalized time. The model predicts the two outputs, unsteady lift and drag coefficients, C_l and C_d . The data is divided into 80% for training, 10% for validation, and 10% for testing. Training data includes $Re \in [1000 - 1500] \cup [2000 - 2500] \cup [3500 - 5000]$. Two values, Re = 1750 and Re = 3000, are used for validation and testing. This is done to check how well the model works



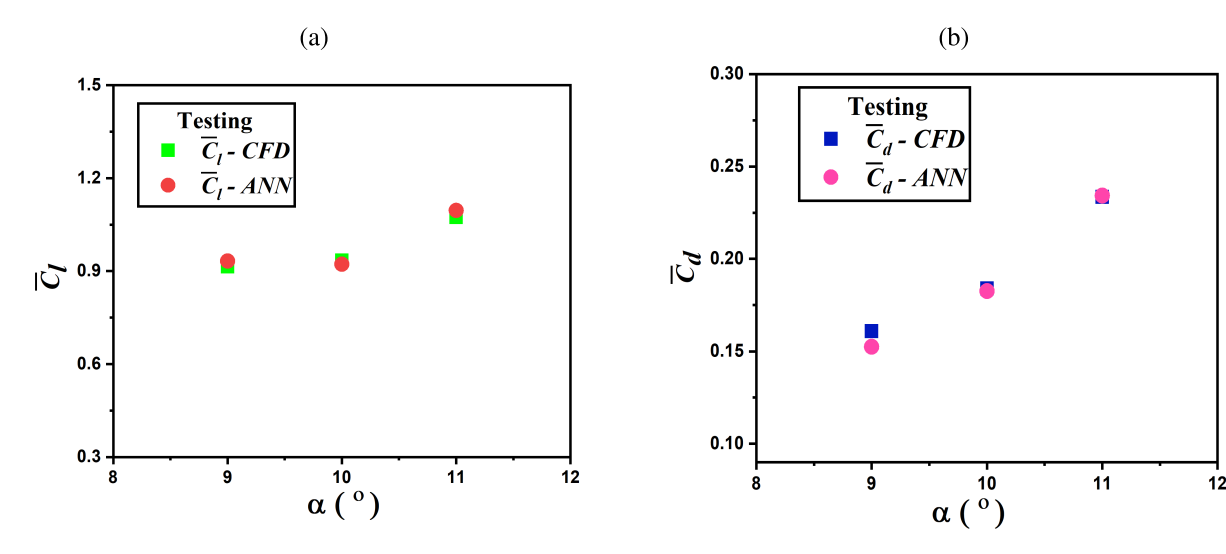


FIGURE 6. CFD and ANN predictions at Re = 3000 (unseen during training) are shown for (a) mean lift coefficient $\overline{C_I}$ and (b) mean drag coefficient $\overline{C_d}$ at selected angles of attack (α).

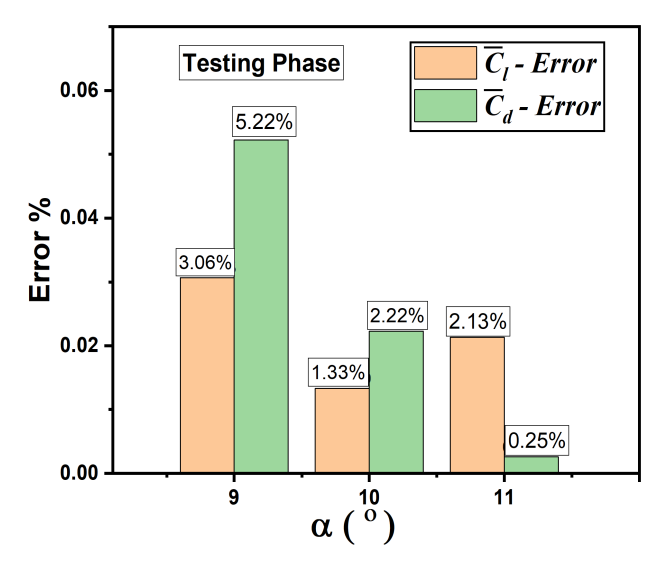


FIGURE 7. Testing phase error percentages for predicted mean lift coefficient (\bar{C}_I) and mean drag coefficient (\bar{C}_d) with respect to CFD results at angles of attack (α) of 9° , 10° , and 11° .

on data it has not seen before. A total of 2777 data points are used in the study.

B. ANN MODELS

The characteristics of data, the complexity of task, and the available computational resources are key factors to consider while selecting a neural network architecture. ANNs consist of various architectures tailored for specific tasks and applications [27], [28], [29]. The simplest form is the perceptron (single-layer architecture) used primarily for binary classification [29]. Although it is simple, it lays the foundation for more complex models, as well as being effective for linearly separable data. ANNs can be categorized based on their complexity. Single-layer feedforward networks only have an input and output layer, with no hidden layers.

These are useful for basic tasks like linear regression but cannot model complex data. Recurrent Neural Networks (RNNs) add memory by using context units, allowing to handle data over time. In comparison to RNNs, LSTM networks are more advanced and handle long-term dependencies more effectively [30]. Radial Basis Function Networks (RBFNs) use radial basis functions as activation functions. These are easier to train than multilayer perceptrons and are good for tasks like function approximation. The structure includes an input layer, a hidden layer with RBF neurons, and an output layer. Adding hidden layers to simpler models leads to multilayered perceptrons (MLPs) [31], [32]. This helps the network learn more complex relationships in data. A common type of MLP is the Feedforward Neural Network (FNN), where information moves in one direction from input to output. A backpropagation algorithm is used to train FNNs, which improves accuracy by adjusting weights.

A Convolutional Neural Network (CNN) [33] is a type of neural network designed specifically for handling gridlike images; it automatically extracts features from grids, making it a highly effective tool for tasks such as object detection and image classification. Furthermore, Deconvolutional Networks are useful in applications such as image segmentation and super-resolution by reconstructing input features from lower-dimensional representations. Another potential architecture in unsupervised learning, self-organizing maps (SOMs) high-dimensional data into low-dimensional spaces while maintaining the topological properties [34]. The number of factors such as data characteristics, task complexity, and available computational resources is required to be carefully considered while selecting a neural network architecture. The strengths and limitations of each architecture need to be carefully aligned with specific requirements. In this study, the Scaled Conjugate Gradient (SCG) algorithm is used for training neural networks due to its efficiency and fast convergence [35]. SCG is considered ideal for limited



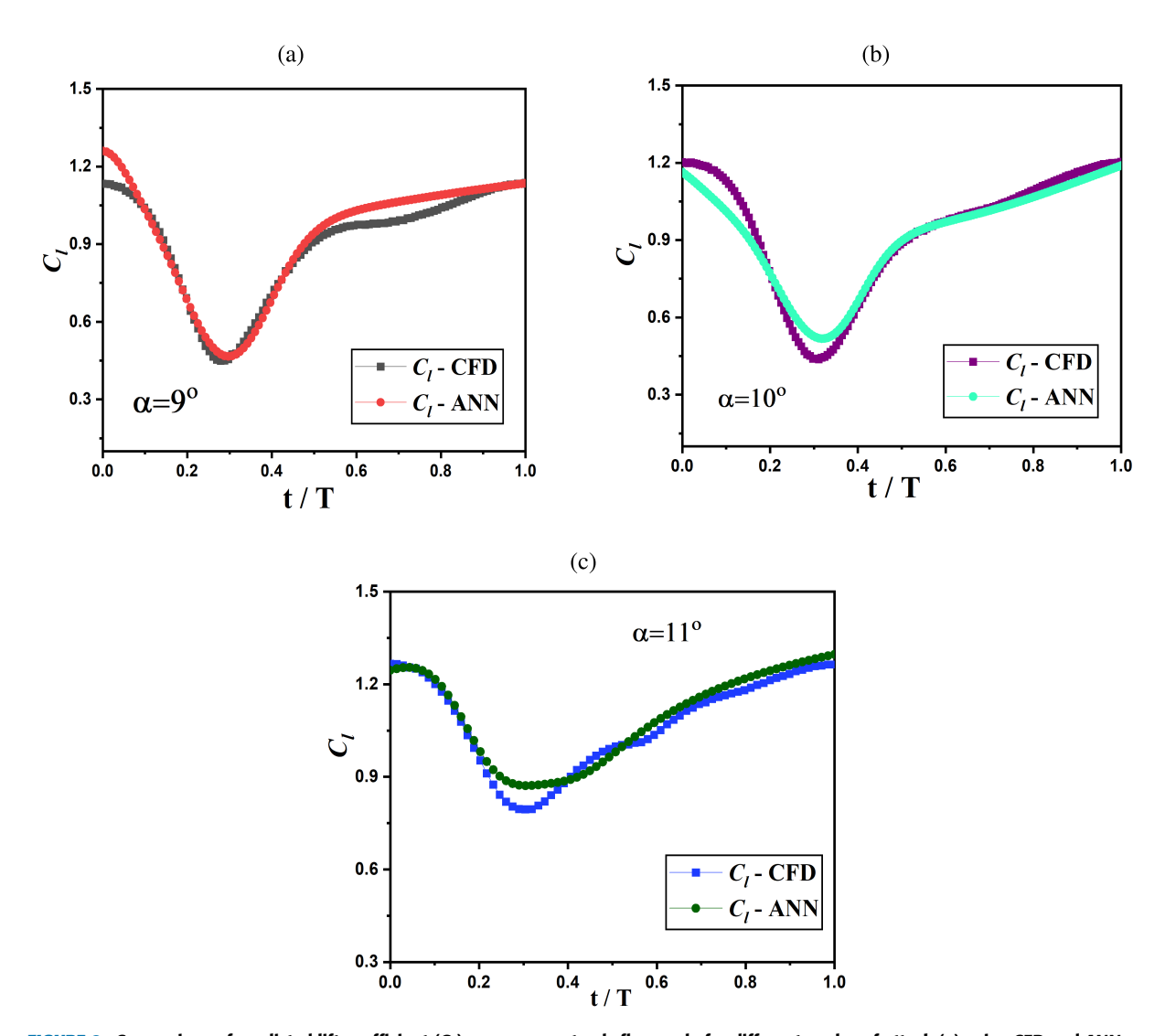


FIGURE 8. Comparison of predicted lift coefficient (C_I) over one unsteady flow cycle for different angles of attack (α) using CFD and ANN models: (a) $\alpha = 9^{\circ}$, (b) $\alpha = 10^{\circ}$, and (c) $\alpha = 11^{\circ}$.

computing resources due to the simplicity and ability to reach solutions in fewer steps. It is also memory-efficient, as it only uses first-order derivatives and avoids storing the full Hessian matrix. The algorithm automatically adjusts the step size and removes the requirement to manually set learning rates. Its ability to handle nonlinear problems makes SCG a reliable choice for neural network optimization.

C. ARCHITECTURE OF THE SCG MODEL

Scaled Conjugate Gradient (SCG) algorithm is employed for training and predicting with ANNs due to its computational efficiency, low memory consumption, and reliable convergence. This makes it well-suited for function approximation tasks such as aerodynamic coefficient prediction. Its capability to effectively capture the nonlinear characteristics of aerodynamic behavior significantly contributed to the predictive performance i camparison to other models. A custom Matlab code has been developed for implementation. SCG is recognized as an effective optimization algorithm in the

field of ANNs, primarily aimed to minimize the error function associated with neural network training. It accomplishes by adjusting various weights and biases to reduce the discrepancy between predicted and actual (CFD) values. The process begins with an initial guess for the parameters, followed by the computation of the gradient of the error function. SCG uses a scaled identity matrix to iteratively improve parameter estimates. To achieve a balance between rapid convergence and stability in optimization, the adaptive scaling of this matrix is essential. The network architecture consists of an input layer, two hidden layers, and an output layer. In this study, the optimal configuration is identified by keeping 9 fixed neurons in first hidden layer and varying the number of neurons in the second hidden layer from 1-100, resulting in outputs closely aligned with computational data.

D. TRAINING ANN

Artificial neural networks for prediction or classification involve a step-by-step process to ensure accurate and reliable



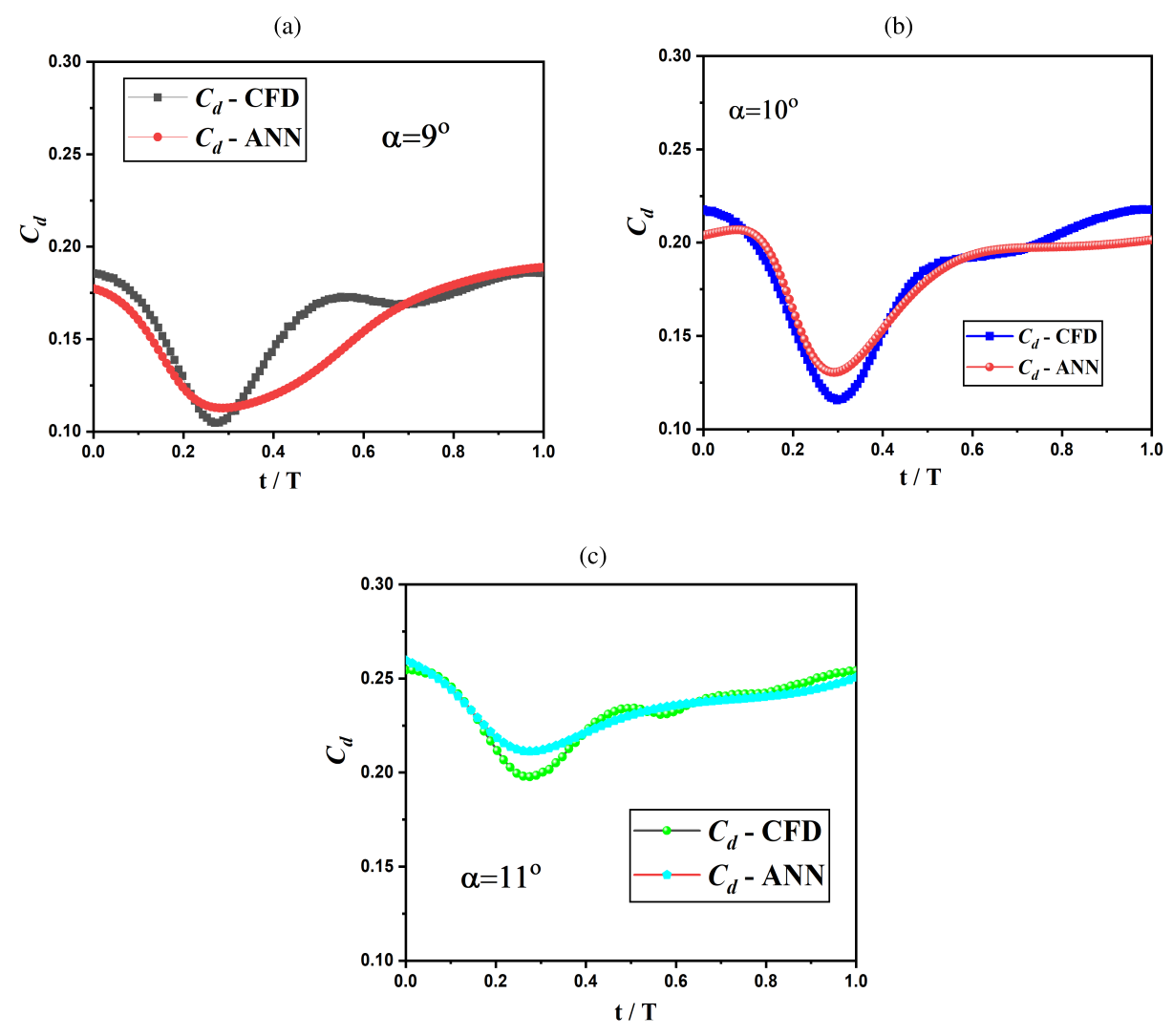


FIGURE 9. Predicted drag coefficient (C_d) over one unsteady flow cycle for different angles of attack (α) using CFD and ANN models: (a) $\alpha = 9^{\circ}$, (b) $\alpha = 10^{\circ}$, and (c) $\alpha = 11^{\circ}$.

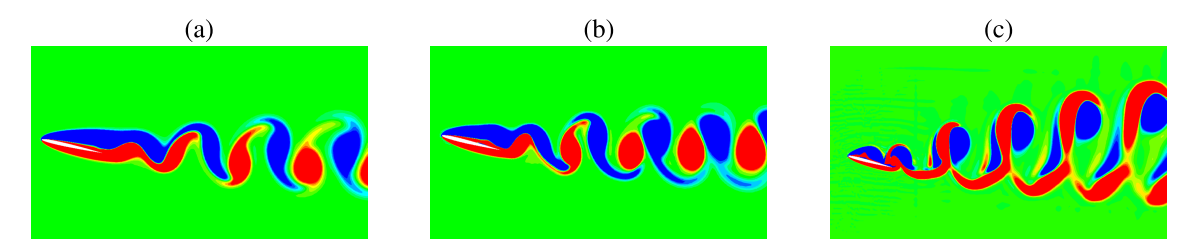


FIGURE 10. Transition of wake at $\alpha=11^{\circ}$ for increasing Reynolds number (a) Re=1000, (b) Re=1500, and (c) Re=3000.

results. An input feature and a target output are used to define the problem. Then, the data is collected, cleaned to remove errors, and normalized so all inputs are on the same scale. The dataset is divided into three parts: a training set to teach the model, a validation set to adjust model settings, and a test set to check performance on new data.

The ANN structure is designed based on the complexity of problem. Hidden layers add non-linearity and allow the model to learn more complex patterns. Activation functions are used in these hidden layers to improve learning. During training, the validation set helps to monitor the model and tune hyperparameters like learning rate or the number of neurons. After training, the test set is used to measure performance using metrics such as accuracy or Mean Absolute Error (MAE). A well-trained model should give accurate results even on data it hasn't seen before.

In this study, the ANN model uses three input variables: angle of attack, Reynolds number, and time. The outputs are unsteady C_l and C_d . The network has two hidden layers. The



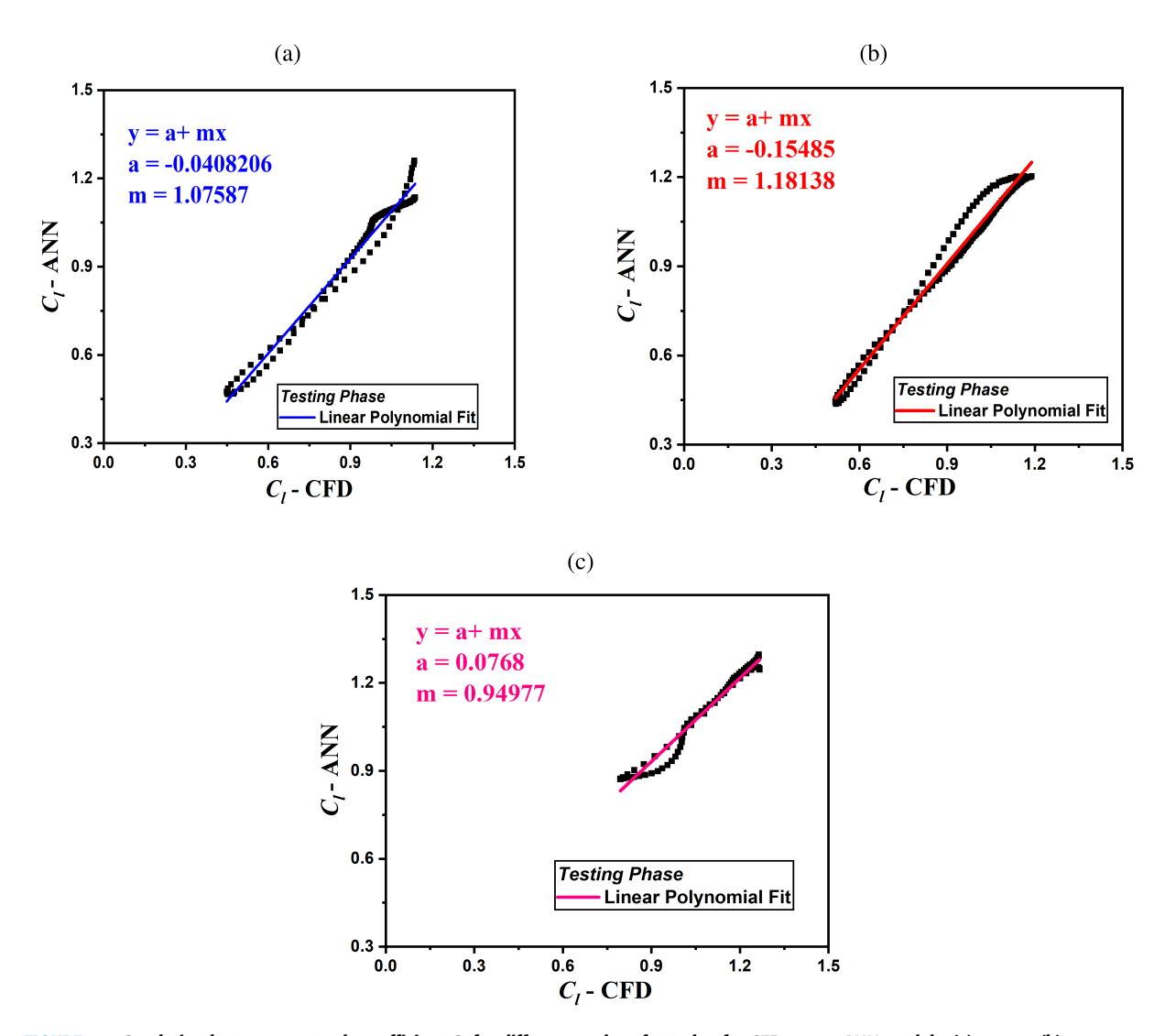


FIGURE 11. Corelation between unsteady coefficient C_I for different angles of attack α for CFD versus ANN models. (a) $\alpha = 9^{\circ}$, (b) $\alpha = 10^{\circ}$, and (c) $\alpha = 11^{\circ}$.

first hidden layer has 9 neurons, while the number of neurons in the second layer varies. Figures 1 and 2 show the ANN setup, and results are provided in Table 1.

E. HARDWARE AND SOFTWARE DETAILS

The CFD and ANN-based approaches for evaluating aero-dynamic properties were conducted using distinct methodologies, hardware, and software setups. For simulations, NACA0005 is modelled and run in Fluent v.22 and Tecplot is used to analyze the data obtained. For the ANN work, a high-performance computing setup was used, featuring a 12th Gen Intel Core i9 CPU, 32 GB RAM, and an NVIDIA GeForce RTX 3080 GPU. MATLAB R2022b was utilized to implement the Scaled Conjugate Gradient (SCG) algorithm. The CFD data collected was split into training (80%), validation (10%), and predicting (10%) subsets. ANN simulations were prompt. The ANN completes a simulation per cycle 5 times faster than CFD. The CFD results were used as a benchmark to assess the performance of the ANN model.

Evaluation metrics such as the coefficient of determination (R^2) , mean squared error (MSE), mean absolute error (MAE), root mean squared error (RMSE), standard deviation (σ) , variance (σ^2) , and error (E) were employed to measure the accuracy of model.

Absolute Error,
$$E_i = |x_{\text{CFD},i} - x_{\text{ANN},i}|$$
 (1)
Error Percentage, $E_i\% = \left(\frac{|x_{\text{CFD},i} - x_{\text{ANN},i}|}{x_{\text{CFD},i}}\right) \times 100\%$ (2)

Mean absolute error, MAE =
$$\frac{1}{n} \sum_{i=1}^{n} |x_{\text{CFD},i} - x_{\text{ANN},i}|$$
 (3)

Mean square error, MSE =
$$\frac{1}{n} \sum_{i=1}^{n} (x_{\text{CFD},i} - x_{\text{ANN},i})^2$$
 (4)

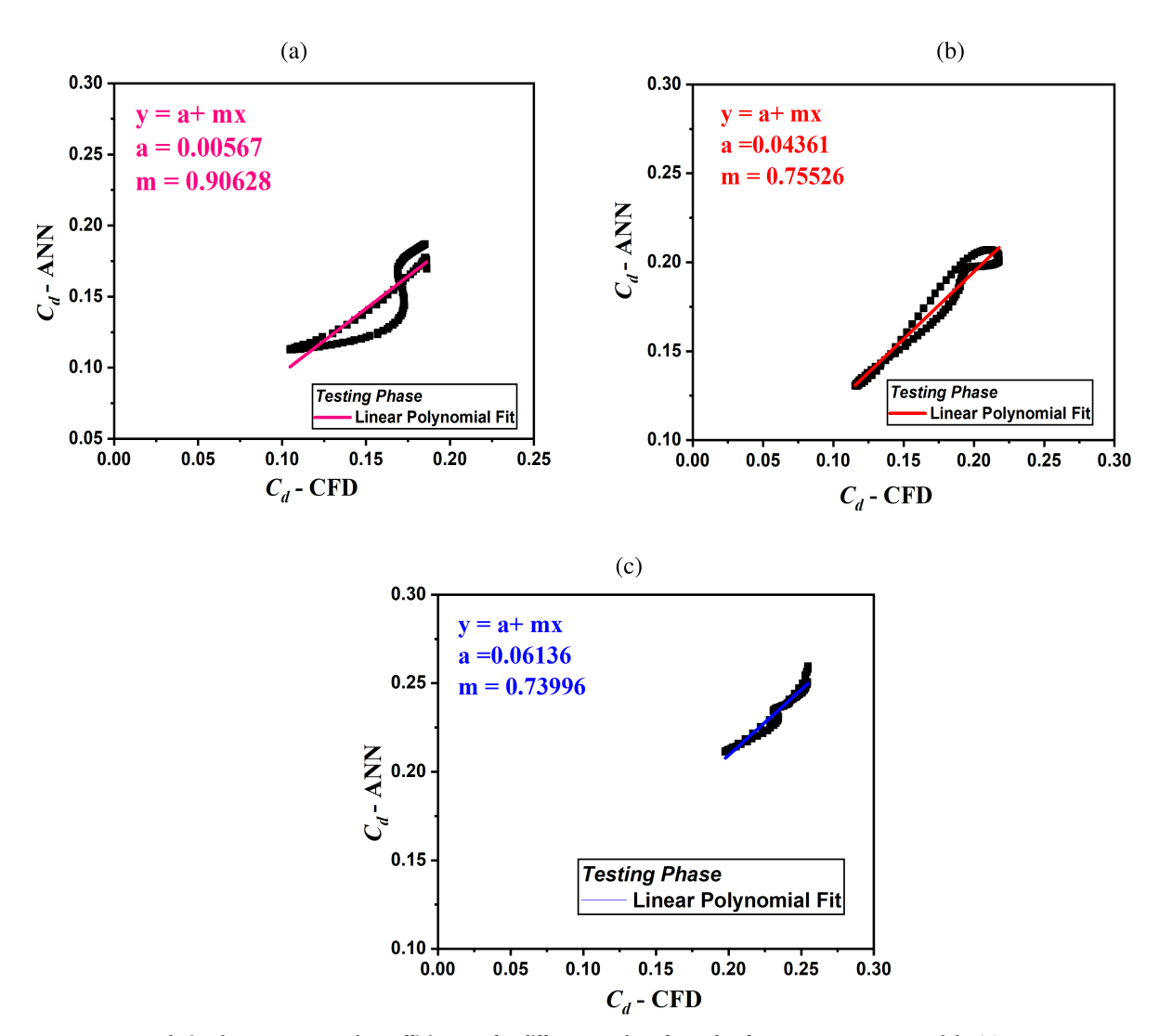


FIGURE 12. Corelation between unsteady coefficient C_d for different angles of attack α for CFD versus ANN models. (a) $\alpha = 9^\circ$, (b) $\alpha = 10^\circ$, and (c) $\alpha = 11^\circ$.

(7)

Root mean square error, RMSE =
$$\sqrt{\frac{1}{n} \sum_{i=1}^{n} (x_{\text{CFD},i} - x_{\text{ANN},i})^2}$$

Standard deviation, $\sigma = \left[\frac{1}{n}\sum_{i=1}^{n}(x_{\text{CFD},i} - \bar{x}_{\text{CFD}})^2\right]^{1/2}$

Variance,
$$\sigma^2 = \frac{1}{n} \sum_{i=1}^{n} (x_{\text{CFD},i} - \bar{x}_{\text{CFD}})^2$$

Coefficient of determination,

$$R^{2} = 1 - \frac{\frac{1}{n} \sum_{i=1}^{n} (x_{\text{CFD},i} - x_{\text{ANN},i})^{2}}{\frac{1}{n} \sum_{i=1}^{n} (x_{\text{CFD},i} - \bar{x}_{\text{CFD}})^{2}}$$
(8)

where, $x_{\text{CFD},i}$ are actual values from CFD at index i, \bar{x}_{CFD} is mean of observed CFD values, $x_{\text{ANN},i}$ are predicted value

from ANN at index i, and n be total number of data points.

III. RESULTS

A detailed evaluation of the performance of the developed artificial neural network (ANN) model is presented in this section for predicting aerodynamic coefficients for the NACA0005 airfoil.

Let

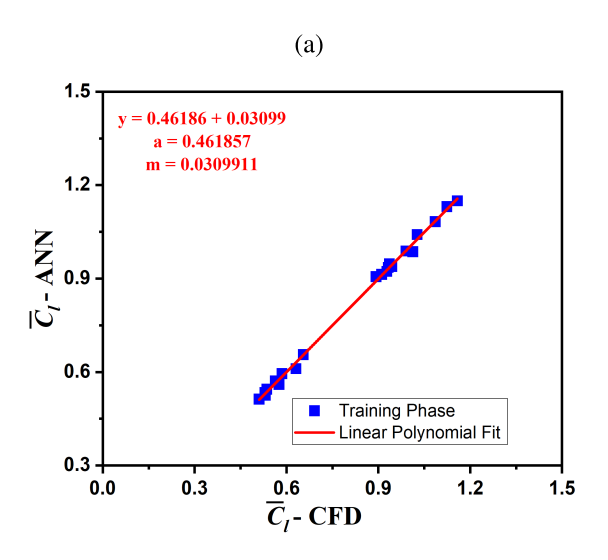
$$A = \begin{bmatrix} a_1 \ a_2 \ a_3 \end{bmatrix}^T \in \mathbb{R}^{3 \times 1}$$

be the input vector. The optimized neural network with two hidden layers contains 9 and 5 neurons respectively, and two outputs C_l and C_d works as:

$$\begin{bmatrix} C_L \\ C_D \end{bmatrix} = \sigma_O \left[W_O \cdot \sigma_2 \left(W_2 \cdot \sigma_1 \left(W_1 \cdot A + B_1 \right) + B_2 \right) + B_O \right]$$
(9)

In explicit matrix form, this becomes:





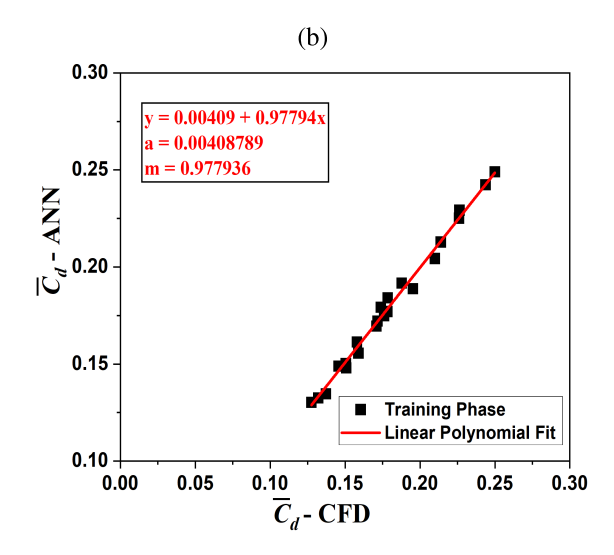


FIGURE 13. ANN-predicted and CFD-computed values for (a) \overline{c}_l and (b) \overline{c}_d during the training phase.

$$\begin{bmatrix}
C_{L} \\
C_{D}
\end{bmatrix} = \sigma_{O} \left(\begin{bmatrix} w_{O}^{11} & \cdots & w_{O}^{15} \\ w_{O}^{21} & \cdots & w_{O}^{25} \end{bmatrix} \right) \\
\cdot \sigma_{2} \left(\begin{bmatrix} w_{2}^{11} & \cdots & w_{2}^{19} \\ \vdots & \ddots & \vdots \\ w_{2}^{51} & \cdots & w_{2}^{59} \end{bmatrix} \cdot \sigma_{1} \left(\begin{bmatrix} w_{1}^{11} & w_{1}^{12} & w_{1}^{13} \\ \vdots & \vdots & \vdots \\ w_{1}^{91} & w_{1}^{92} & w_{1}^{93} \end{bmatrix} \right) \\
\cdot \begin{bmatrix} a_{1} \\ a_{2} \\ a_{3} \end{bmatrix} + \begin{bmatrix} b_{1}^{(1)} \\ \vdots \\ b_{9}^{(1)} \end{bmatrix} + \begin{bmatrix} b_{1}^{(2)} \\ \vdots \\ b_{5}^{(2)} \end{bmatrix} + \begin{bmatrix} b_{1}^{(O)} \\ b_{2}^{(O)} \end{bmatrix} \right). \tag{10}$$

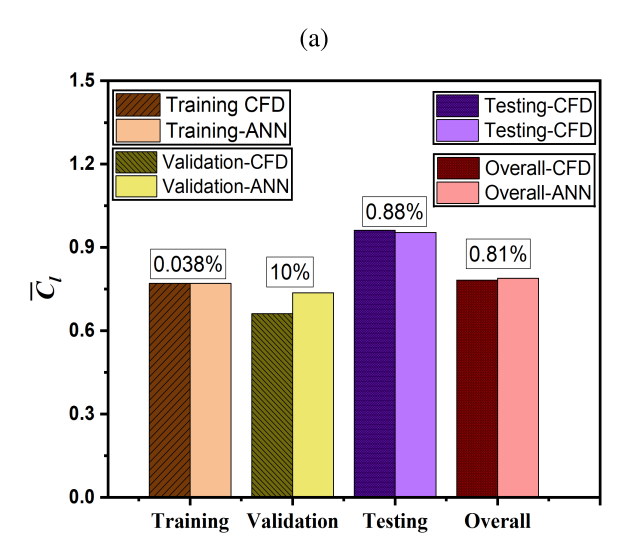
where.

- $A \in \mathbb{R}^3$: Input characteristic vector consists of a_1 , a_2 , and a_3 as aerodynamic parameters such as angle of attack, Reynolds number, and Mach number.
- $W_1 \in \mathbb{R}^{9 \times 3}$: Weight matrix between the input layer and the first hidden layer (9 neurons).
- $B_1 \in \mathbb{R}^9$: Bias vector added to the first hidden layer.
- σ_1 : Activation function applied to the first hidden layer.
- $W_2 \in \mathbb{R}^{5 \times 9}$: Weight matrix between the first and second hidden layers (5 neurons).
- $B_2 \in \mathbb{R}^5$: Bias vector for the second hidden layer.
- σ_2 : Activation function for the second hidden layer.
- $W_O \in \mathbb{R}^{2 \times 5}$: Weight matrix between the second hidden layer and the output layer (2 outputs: C_L and C_D).
- $B_O \in \mathbb{R}^2$: Bias vector for the output layer.
- σ_O : Final activation function applied to the output.

Figure 3 (a and b) shows the distribution of coefficient of determination (R^2) values for neural network models used to predict the C_l and C_d . Each model uses a two-layer architecture, with 9 neurons fixed in the first hidden layer. The number of neurons in the second hidden layer varies from 1 to 100. Each vertical bar represents the R^2 value for a specific number of neurons in the second layer. The results show that prediction accuracy changes

significantly with the number of neurons. Although several configurations achieve high R^2 values, these peaks are not consistent across both output variables. Several neurons that yield strong performance for C_l often underperform for C_d , and vice versa. To address this, the 10 best neurons are selected based on balanced performance for both C_l and C_d , instead of focusing on one alone parameter (Table 1). This approach ensures the models are reliable for predicting both coefficients. Among these, the ANN with five neurons showed accurate and balanced predictions for both lift and drag coefficients. It achieved high R^2 values as 0.994 and 0.9563 for C_l on the training and testing sets, and 0.9615 and 0.9085 for C_d . It shows that the model is reliable for both outputs.

To check the accuracy of the ANN predictions, the mean results were compared directly with CFD simulations results for each set of training, validation and testing. Figures 4 to 6 show these comparison between mean values of CFD and ANN for selected angles of attacks $\alpha = 9^{\circ}$, 10° , and 11° . In Figure 4, the ANN results (training phase) are compared with CFD. At $\alpha = 9^{\circ}$, the ANN results are highly accurate as in close agreement with the CFD data. At $\alpha = 10^{\circ}$, the model still predicts $\overline{C_l}$ well, but $\overline{C_d}$ shows some discrepancies with lower percentage errors. At $\alpha = 11^{\circ}$, both $\overline{C_l}$ and $\overline{C_d}$ predictions are again closely align with the CFD results. To test how well the ANN generalizes to new cases, data for Reynolds numbers Re = 1750 and Re = 3000 were left out of training. The model was then tested on these cases: Re = 1750 was used for validation and Re = 3000 for testing, as shown in figures 5 and 6. For Re = 1750, the ANN performed very well at $\alpha = 9^{\circ}$ and 10° . It proves that the method has the capability to predict lift and drag coefficients accurately in linear wake regimes. At $\alpha = 11^{\circ}$, the ANN slightly underpredicts, due to complex flow behavior that was not well represented in the training data with errors as much high as 10%.



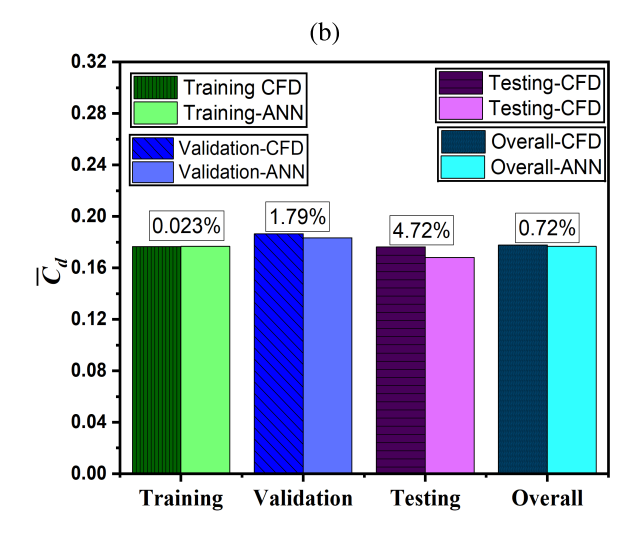


FIGURE 14. Overall percentage error in mean lift $(\overline{C_l})$ and drag $(\overline{C_d})$ coefficients predicted by CFD and ANN models across the training, validation, testing, and overall datasets. (a) Error in $\overline{C_l}$: (b) Error in $\overline{C_d}$.

The results for Re = 3000, which was not used during training is presented in figures 6-11. It is crucial to investigate testing phase in detail for successful ANN network implementation. In figure 6(a) The predictions are very close to the CFD data, especially at $\alpha = 9^{\circ}$ and 10° , indicating high accuracy. At $\alpha = 11^{\circ}$, the ANN slightly overpredicts the mean lift coefficient by 2.13%, and the error in mean C_d is negligible as 0.25% (figure 7). Figure 6(b) shows the drag coefficient comparison, where the ANN predictions closely follow the CFD results. A slight underprediction is observed at $\alpha = 9^{\circ}$, though the overall trend remains consistent. For instance, at $\alpha = 10^{\circ}$ and 11° , the values match very well to CFD results. Overall, the ANN model accurately captures aerodynamic behavior, even for test cases outside the training data. This confirms its effectiveness and reliability as a fast alternative to CFD simulations within this operating range. Figures 8 and 9 present a comparison between the predictions of the ANN model and CFD simulation results for the unsteady C_l and C_d , respectively, over a full motion cycle (t/T) at three angles of attack 9° , 10° , and 11° .

In figure 8 (unsteady C_l), the ANN model performs well across all angles. At $\alpha=9^\circ$, the ANN predictions align closely with the CFD results, accurately captures both the shape and magnitude of the lift curve. At $\alpha=10^\circ$, the agreement remains strong, with only slight deviations observed near the minimum point of the curve. For $\alpha=11^\circ$, the ANN continues to follow the overall trend of the CFD data, although minor discrepancies become more apparent, particularly near the minimum values. These differences are likely due to increased nonlinear flow behavior at higher angles. Similar comparison for unsteady C_d is presented in figure 9. At $\alpha=9^\circ$, the ANN accurately predicts the C_d values, closely follow the CFD trend. At $\alpha=10^\circ$, the ANN slightly underestimates the C_d near the minimum point, but the general pattern and timing remain consistent with CFD.

For $\alpha=11^{\circ}$, while the ANN captures the overall behavior of the curve, noticeable deviations occur in some parts, possibly due to more complex flow features like separation or transition (Figure 10).

Overall, the ANN model shows strong potential in predicting both unsteady pattern of lift and drag coefficients. Its predictions are highly accurate at lower and moderate angles of attack, where the flow is mostly linear and attached. Although the accuracy slightly decreases at higher angles due to nonlinear effects, the model still captures the main aerodynamic trends throughout the cycle.

A strong linear correlation between the coefficients (C_l and C_d) predicted by an ANN and those computed using CFD at three angles of attack: 9° (a), 10° (b), and 11° (c) are observed (figures 11 and 12). The data corresponds to unsteady flow conditions over a single oscillation cycle. Each subplot includes a linear fit of the form y = a + mx, which captures the relationship between ANN predictions and CFD results. All three cases indicate that the ANN is capable of accurately learning the unsteady aerodynamic behavior from CFD data. The variations reflect the sensitivity of ANN performance to changes in flow conditions and angle of attack. Similarly, the correlation for training data is plotted in figure 13. Plotting individual cases was avoided to maintain clarity, and mean values were used instead. Figure 13(a and b), the high correlation reflects effective learning of drag behavior across the training conditions.

Figure 14 illustrates the overall performance by percentage error between ANN and CFD predictions across different cases. In general, the ANN predictions align closely with the CFD results, particularly when the flow is attached and remains two-dimensional. The only notable deviation occurs during the validation phase at $\alpha=11^\circ$, likely caused by alterations in the flow behavior behind the airfoil. Overall, the ANN model proves to be a fast and accurate



tool for predicting aerodynamic performance at lower angles of attack. The percentage errors are generally low, such as 0.038% for $\overline{C_l}$ and 0.023% for $\overline{C_d}$ during training, demonstrating the model's ability to learn CFD patterns effectively. While slightly higher errors are observed during validation and testing—10% and 0.88% for $\overline{C_l}$. However, for $\overline{C_d}$, the error becomes lower as 1.79% and 4.72%. The overall differences remain minimal, typically below 1%, confirming the ANN's consistency in approximating CFD outputs for ultra-low Reynolds numbers.

IV. CONCLUSION AND LIMITATIONS

In this study, Scaled Conjugate Gradient (SCG) algorithm is applied to an ANN to predict the time-averaged aerodynamic coefficients of a NACA0005 airfoil. The performance of the SCG algorithm is validated by statistical metrics that highlight the accuracy and reliability of the ANN predictions. The ANN demonstrated excellent predictive performance for unsteady C_l and C_d coefficients within selected range of the Reynolds numbers 1000 - 5000 and angles of attack 9° to 11° as well as for mean values. Parametric optimization of the network architecture revealed that a two-layer feedforward network with nine neurons in the first hidden layer and five in the second layer is sufficient to achieve high correlation with CFD benchmarks ($R^2 > 0.99$ and 0.96 for training and 0.95 along with 0.91 in testing phase) for unsteady C_l and C_d respectively. The ANN successfully generalized to untrained Reynolds numbers (Re = 1750 and Re = 3000), with error margins below 2% in most cases except 11°. It confirms the ability of ANN to interpolate within the defined input space. Furthermore, the ANN captured both steady and unsteady aerodynamic trends. Although minor deviations were observed at $\alpha = 11^{\circ}$ likely due to increased flow separation and nonlinear wake interactions. However, this work has some limitations and needs to address:

Limitations and Future Work: The current model is limited to 2D, incompressible, laminar flow conditions and is trained on data from a single symmetric airfoil. As such, its extrapolation capabilities beyond the trained domain (e.g., compressible regimes, 3D effects, high-angle stall) are inherently constrained. Future extensions will include the integration of broader datasets encompassing several airfoil geometries, Mach numbers, and turbulent flow regimes. Incorporating hybrid surrogate-CFD frameworks could further enhance model fidelity, particularly in nonlinear flow regimes. In addition, embedding uncertainty quantification methods will be essential for real-world deployment in design optimization and active flow control applications.

ACKNOWLEDGMENT

The authors thank the King Abdullah University of Science and Technology (KAUST), the Supercomputing Laboratory, and HPC Resources (KAUST) for providing computing resources.

REFERENCES

- [1] M. Dildar, S. Akram, M. Irfan, H. U. Khan, M. Ramzan, A. R. Mahmood, S. A. Alsaiari, A. H. M. Saeed, M. O. Alraddadi, and M. H. Mahnashi, "Skin cancer detection: A review using deep learning techniques," *Int. J. Environ. Res. Public Health*, vol. 18, no. 10, p. 5479, 2021.
- [2] A. Krogh, "What are artificial neural networks?" Nature Biotechnol., vol. 26, no. 2, pp. 195–197, Feb. 2008.
- [3] J. F. Zapata Usandivaras, A. Urbano, M. Bauerheim, and B. Cuenot, "Data driven models for the design of rocket injector elements," *Aerospace*, vol. 9, no. 10, p. 594, Oct. 2022.
- [4] B. Jang, W. Lee, J.-J. Lee, and H. Jin, "Artificial neural network-based temperature prediction of a lunar orbiter in thermal vacuum test: Datadriven reduced-order models," *Aerosp. Sci. Technol.*, vol. 145, Feb. 2024, Art. no. 108867.
- [5] S. Keshmiri, R. Colgren, and M. Mirmirani, "Development of an aerodynamic database for a generic hypersonic air vehicle," in *Proc. AIAA Guid., Navigat., Control Conf. Exhibit*, Aug. 2005, p. 6257.
- [6] M. Ghoreyshi, R. M. Cummings, A. D. Ronch, and K. J. Badcock, "Transonic aerodynamic load modeling of X-31 aircraft pitching motions," *AIAA J.*, vol. 51, no. 10, pp. 2447–2464, Oct. 2013.
- [7] E. Z. Abyaneh, F. Ein-Mozaffari, and A. Lohi, "Critical review of gas-liquid mixing using gas-inducing impellers: Modeling, CFD simulation, and ANN applications," *Ind. Eng. Chem. Res.*, vol. 63, no. 35, pp. 15325–15350, 2024.
- [8] S. L. Brunton, B. R. Noack, and P. Koumoutsakos, "Machine learning for fluid mechanics," *Annu. Rev. Fluid Mech.*, vol. 52, no. 1, pp. 477–508, Jan. 2020.
- [9] L. Hu, J. Zhang, Y. Xiang, and W. Wang, "Neural networks-based aerodynamic data modeling: A comprehensive review," *IEEE Access*, vol. 8, pp. 90805–90823, 2020.
- [10] B. Wang, S. Ma, H. Zhou, Q. Zheng, W. Lan, S. Jing, and S. Li, "A CFD-PBM-ANN framework to simulate the liquid-liquid two-phase flow in a pulsed column," AIChE J., vol. 71, no. 1, p. 18612, Jan. 2025.
- [11] R. M. Greenman and K. R. Roth, "High-lift optimization design using neural networks on a multi-element airfoil," in *Proc. Volume 6: 18th Comput. Eng. Conf.*, Sep. 1998, p. 006.
- [12] T. Duriez, S. L. Brunton, and B. R. Noack, *Machine Learning Control-taming Nonlinear Dynamics and Turbulence*, vol. 116. Cham, Switzerland: Springer, 2017.
- [13] M. P. Brenner, J. D. Eldredge, and J. B. Freund, "Perspective on machine learning for advancing fluid mechanics," *Phys. Rev. Fluids*, vol. 4, no. 10, Oct. 2019, Art. no. 100501.
- [14] D. F. Kurtulus, "Unsteady aerodynamics of a pitching NACA 0012 airfoil at low Reynolds number," *Int. J. Micro Air Vehicles*, vol. 11, Jan. 2019, Art. no. 1756829319890609.
- [15] T. Kouser, Y. Xiong, D. Yang, and S. Peng, "Direct numerical simulations on the three-dimensional wake transition of flows over NACA0012 airfoil at re = 1000," *Int. J. Micro Air Vehicles*, vol. 13, Jan. 2021, Art. no. 17568293211055656.
- [16] D. F. Kurtulus, "On the wake pattern of symmetric airfoils for different incidence angles at re = 1000," *Int. J. Micro Air Vehicles*, vol. 8, no. 2, pp. 109–139, Jun. 2016.
- [17] G. Catalani, D. Costero, M. Bauerheim, L. Zampieri, V. Chapin, N. Gourdain, and P. Baqué, "A comparative study of learning techniques for the compressible aerodynamics over a transonic RAE2822 airfoil," *Comput. Fluids*, vol. 251, Jan. 2023, Art. no. 105759.
- [18] M.-Y. Wu, Y. Wu, X.-Y. Yuan, Z.-H. Chen, W.-T. Wu, and N. Aubry, "Fast prediction of flow field around airfoils based on deep convolutional neural network," *Appl. Sci.*, vol. 12, no. 23, p. 12075, Nov. 2022.
- [19] J. Kou and W. Zhang, "Layered reduced-order models for nonlinear aerodynamics and aeroelasticity," J. Fluids Struct., vol. 68, pp. 174–193, Jan. 2017.
- [20] D. F. Kurtulus, "Ability to forecast unsteady aerodynamic forces of flapping airfoils by artificial neural network," *Neural Comput. Appl.*, vol. 18, no. 4, pp. 359–368, May 2009.
- [21] Y. Zhang, W. J. Sung, and D. N. Mavris, "Application of convolutional neural network to predict airfoil lift coefficient," in *Proc. AIAA/ASCE/AHS/ASC Struct., Structural Dyn., Mater. Conf.*, Jan. 2018, p. 1903.



- [22] A. Usman, M. Rafiq, M. Saeed, A. Nauman, A. Almqvist, and M. Liwicki, "Machine learning computational fluid dynamics," in *Proc. Swedish Artif. Intell. Soc. Workshop (SAIS)*, Jun. 2021, pp. 1–4.
- [23] E. Ajuria Illarramendi, A. Alguacil, M. Bauerheim, A. Misdariis, B. Cuenot, and E. Benazera, "Towards an hybrid computational strategy based on deep learning for incompressible flows," in *Proc. AIAA AVIATION FORUM*, Jun. 2020, p. 3058.
- [24] T. Kouser, D. F. Kurtulus, A. Aliyu, S. Goli, L. M. Alhems, I. H. Imran, and A. M. Memon, "Unsteady aerodynamics over NACA0005 airfoil for ultra-low Reynolds numbers," *IEEE Access*, vol. 12, pp. 83658–83674, 2024.
- [25] S. Goli, D. F. Kurtuluş, M. Waqar, I. H. Imran, L. M. Alhems, T. Kouser, and A. M. Memon, "Artificial neural network for the evaluation of electric propulsion system in unmanned aerial vehicles," *Neural Comput. Appl.*, vol. 37, no. 15, pp. 1–17, May 2025.
- [26] M. F. Møller, "A scaled conjugate gradient algorithm for fast supervised learning," *Neural Netw.*, vol. 6, no. 4, pp. 525–533, Jan. 1993.
- [27] C. M. Bishop, Neural Networks for Pattern Recognition. London, U.K.: Oxford Univ. Press. 1995.
- [28] E. Guresen and G. Kayakutlu, "Definition of artificial neural networks with comparison to other networks," *Proc. Comput. Sci.*, vol. 3, pp. 426–433, Jan. 2011.
- [29] E. Alpaydin, Introduction To Machine Learning. Cambridge, MA, USA: MIT Press, 2020.
- [30] N. T. Luchia, E. Tasia, I. Ramadhani, A. Rahmadeyan, and R. Zahra, "Performance comparison between artificial neural network, recurrent neural network and long short-term memory for prediction of extreme climate change," *Public Res. J. Eng., Data Technol. Comput. Sci.*, vol. 1, no. 2, pp. 62–70, Feb. 2024.
- [31] K. Y. Chan, B. Abu-Salih, R. Qaddoura, A. M. Al-Zoubi, V. Palade, D.-S. Pham, J. D. Ser, and K. Muhammad, "Deep neural networks in the cloud: Review, applications, challenges and research directions," *Neurocomputing*, vol. 545, Aug. 2023, Art. no. 126327.
- [32] J. A. Rodrigues, J. T. Farinha, M. Mendes, R. J. G. Mateus, and A. J. M. Cardoso, "Comparison of different features and neural networks for predicting industrial paper press condition," *Energies*, vol. 15, no. 17, p. 6308, Aug. 2022.
- [33] S. Davidson and S. B. Furber, "Comparison of artificial and spiking neural networks on digital hardware," *Frontiers Neurosci.*, vol. 15, Apr. 2021, Art. no. 651141.
- [34] T. Kohonen, "The self-organizing map," Proc. IEEE, vol. 78, no. 9, pp. 1464–1480, 1990.
- [35] T. Ku and Y.-D. Lin, "A computationally efficient algorithm for estimating respiratory rate from seismocardiogram," *Biomed. Signal Process. Control*, vol. 109, Nov. 2025, Art. no. 108030.



DILEK FUNDA KURTULUS received the B.S. and M.S. degrees in aerospace engineering from Middle East Technical University, Ankara, Türkiye, in 2000 and 2002, respectively, and the Ph.D. degree in aerospace engineering from the ENSMA/Université de Poitiers, Poitiers, France. In 2006, she was Postdoctoral Researcher with the Laboratoire d'Etudes Aérodynamique, ENSMA Poitiers, and the Laboratoire de Combustion et Systèmes Réactifs, CNRS, Orléans, France. Since

2018, she has been a Professor with the Department of Aerospace Engineering, Middle East Technical University. Her research interests include aircraft design, unsteady aerodynamics, and autonomous air vehicles. She was a recipient of the Amelia Earhart Fellow at Zonta International, in 2005; the NATO Scientific Achievement Award, in 2011; the Turkish Academy of Science Young Scientific Award, in 2012; and the Zonta International Centennial Recognition Award of Türkiye, in 2019.



SRIKANTH GOLI was born in Hyderabad, India. He received the B.Tech. degree in aeronautical engineering from Jawaharlal Nehru Technological University, in 2008, the M.E. degree in aeronautical engineering from the Hindustan Institute of Technology and Science, in 2011, and the Ph.D. degree from the Department of Aerospace Engineering, IIT Kharagpur, India, in 2019. From 2019 to 2022, he carried out research at various academic institutions and industries. He is

currently a Postdoctoral Researcher with the Applied Research Center for Metrology, Standards, and Testing (ARC-MST), King Fahd University of Petroleum and Minerals (KFUPM), Saudi Arabia. His research interests include aircraft design, experimental and numerical fluid dynamics, and autonomous air vehicles. He has memberships in professional societies, such as the National Society of Fluid Mechanics and Fluid Power, Indian Society of Theoretical and Applied Mechanics, and the Aeronautical Society of India.



TAIBA KOUSER was born in Faisalabad, Pakistan. She received the Ph.D. degree from the School of Aerospace Engineering, Huazhong University of Science and Technology, Wuhan, China, in 2021. Currently, she is a Postdoctoral Researcher with the Applied Research Center for Metrology, Standards, and Testing (ARC-MST), King Fahd University of Petroleum and Minerals (KFUPM), Dhahran, Saudi Arabia. Her area of research is computational fluid dynamics. Her research

interests include drag reduction, unsteady aerodynamics, and aeroacoustics.



ABDULRAHMAN ALIYU received the B.Eng. degree in electrical engineering from Bayero University, Kano, Nigeria, in 2010, and the M.S. and Ph.D. degrees in systems and control engineering from the King Fahd University of Petroleum and Minerals, in 2016 and 2020, respectively. He is currently a Postdoctoral Fellow with the Applied Research Center for Metrology, Standards and Testing, King Fahd University of Petroleum and Minerals. His research interests include robotics,

control theory, multi-agent/large-scale systems, artificial intelligence, energy harvesting, metrology, and sensors.





IMIL HAMDA IMRAN received the B.S. degree in electrical engineering from Andalas University, Indonesia, in 2011, the M.S. degree in systems and control engineering from the King Fahd University of Petroleum and Minerals, Saudi Arabia, in 2015, and the Ph.D. degree in electrical engineering from The University of Newcastle, Australia, in 2020. He was a Postdoctoral Research Associate with the Department of Engineering, Lancaster University, U.K., in 2022. He was a Postdoctoral Researcher

at Lancaster University, U.K., and King Fahd University of Petroleum and Minerals, Saudi Arabia, from 2020 to 2024. He is currently an Assistant Professor with the Department of Electrical Engineering, King Faisal University, Saudi Arabia. His research interests include networked control systems, multi-agent systems, nonlinear control, and adaptive control.



LUAI M. ALHEMS received the Ph.D. degree from Texas A&M University, College Station, TX, USA, in 2002. He is currently a Professor of thermo-fluid with the Department of Mechanical Engineering, King Fahd University of Petroleum and Minerals (KFUPM), Dhahran, Saudi Arabia. He is also the Director of the Applied Research Center for Metrology, Standards, and Testing (ARC-MST) Research Institute. Regional authorities have recognized him for his research work.

He has authored or co-authored more than 180 journal articles and patents. His research interests include gas turbines, energy systems, failure analysis, wind energy, and energy conservation.



AZHAR M. MEMON was born in Pakistan, in 1987. He received the B.E. degree in electronics from the National University of Sciences and Technology (NUST), Pakistan, in 2009, the M.Sc. degree in automation and control engineering from the National University of Singapore (NUS), Singapore, in 2010, and the Ph.D. degree from the King Fahd University of Petroleum and Minerals (KFUPM), Saudi Arabia, in 2015. From 2009 to 2010, he was a Research Engineer

with NUS and a Lecturer, in 2011. He joined the Research and Development Department, Rosen Group, as a Sensors and Algorithm Specialist. In 2019, he joined KFUPM as an Assistant Professor, where he is actively participating in managing various client-funded and internally funded research projects and teaching. He has authored or co-authored several peer-reviewed research articles and conference papers in reputable journals and international conferences. His research interests include control systems, signal processing, data analytics, nondestructive testing, and aquaponics. Website: www.azharmemon.com

0 0 0